Fabrication and Characterization of Polymer Nanocomposites using $BaTiO_3$ Nanoparticles for Optoelectronic Applications

Duaa S. Shakir [1]
Bahaa H. Rabee [1]
Ibtihal M. Al-Hussaini [2]

[1] *Department of Physics, College of Education for Pure Sciences, University of Babylon, Hilla, IRAQ*
[2] *Department of Biology, College of Science, University of Babylon, Hilla, IRAQ*

The hybrid nanomaterials incorporated into organic polymers show promising potential for use in a range of optical and electronics applications. In this study, nanocomposite films made from carboxymethyl cellulose (CMC) filled with nickel oxide (NiO), fig milk, and varying percentages of barium titanate ($BaTiO_3$) nanoparticles were synthesized using a solution casting method. The resulting products were effectively analyzed using Fourier Transform Infrared (FT-IR) spectroscopy and Optical Microscopy (OM). FT-IR analysis verified the existence of functional groups in the polymer nanocomposite structures. UV-visible spectroscopy was utilized to examine the optical properties. The values of indirect allowed and forbidden transition energy gaps decreased with the increasing of $BaTiO_3$ NPs content. The amount of additives also influenced all other measured parameters. These findings suggest that CMC/NiO, fig milk, and $BaTiO_3$ nanocomposites have potential as crucial nanomaterials in the fields of optics and electronics.

Keywords: Nanocomposites; Nanoparticles; Barium Titanate; Optical properties
Received: 18 May 2024; Revised: 16 June 2024; Accepted: 23 June 2024

1. Introduction

Polymers have infiltrated every aspect of our life. In recent years, advancements in understanding the relationship between polymer structure and properties, the innovation of new polymerization techniques, and the increased availability of unique and inexpensive monomers have all played a role in making the idea of creating a customized polymer a viable option [1,2]. Polymers are at the core of the ongoing materials science and technological advancements [3,4]. The electronic industry makes extensive use of dielectric materials with high permittivity [5]. Polymers are used as insulating materials more frequently than traditional insulators such as ceramics due to their superior characteristics such as easy production, flexible mechanical properties, and a relatively high electrical breakdown threshold. Moreover, adding inorganic components to them might change their characteristics [6]. The most common type of cellulose is carboxymethyl cellulose (CMC). Cellulose is a linear, large molecular weight polymer that is a renewable and biodegradable plant material. Although the hydrogen bonds associated with the formation of molecular cellulose does not dissolve quickly or dissolve in certain solvents. However, its soluble forms of water are used for various purposes [7]. Barium titanate ($BaTiO_3$) is a member of the perovskite family, which has several compounds with the same general formula (ABO_3), where the letters A and B stand for divalent and tetravalent cations, which was used for more than 60 years [8]. It is among the most used ceramic electrical components. The beneficial traits it possesses include being a reasonably clear crystalline material, having ferroelectric properties at room temperature, and being a polycrystalline ceramic that is simple to prepare. Barium titanate's high dielectric constant makes it a popular material for capacitors. Among other things, it may be utilized for underwater detection, gas lighters, ultrasonic ventilation, and medical imaging [9,10]. NiO is with a wide band gap of 3.6 eV NiO promising material for variety applications, such as solar thermal absorber. However it is difficult to find a sufficient stable semiconductor device with an adequate band gap for visible absorption. Thus in order to minimize the energy gap, the substrate temperature must be increased and the Cu must be increased in order to obtain an adequate energy gap [11,12]. The addition of fig milk, which acts as an antifungal substance, enhances the role of nanocomposites in the field of optoelectronics.

In this work, CMC/NiO – Fig Milk and different weight percentages of $BaTiO_3$ nanoparticles were synthesized using the solution casting method, and their optical and textural characteristics were studied and discussed.

2. Experimental Part

The polymer carboxy methyl cellulose (CMC) substance used is a white powder, and the molecular weight is 1.7×10^4 g/mol and obtainable from local retailers, with good purity (99.97 %). Fig milk was obtained from a farm in the city of Al-Hilla in Babil Governorate. Nickel oxide (NiO) with particle diameter 30-45 nm cubic phase was obtained from US Research Nanomaterials Inc. with high purity (99.95%). Barium Titanate ($BaTiO_3$) nanopowder was purchased from the local market with density of 6.02 g/cm^3 supplied by US Research Nanomaterials Inc. with high purity ($BaTiO_3$, 99.9%, 50 nm, cubic).

Films of nanocomposites consisting of polymer CMC, NiO/fig milk, and different weight percentages of $BaTiO_3$ NPs were prepared using the solution casting method. The fig milk was dried in the oven at a temperature of 50 °C for 24 hours to transform it from liquid to powder. Then 1g of CMC was dissolved in 40 ml of deionized water. The solution was prepared by mixing on a magnetic stirrer for 30 minutes at a temperature range of 70-80 °C. Subsequently, the solvent and solution were transferred to a Petri dish and allowed to gently evaporate at room temperature for 168 hours. Once removed from the Petri dish, the synthesized dry film was stored in vacuum desiccators. Nanocomposite (NCs) films were prepared from CMC with 3 wt.% Fig Milk, 3 wt.% NiO, and varying percentages (1, 2, 3, 4) of $BaTiO_3$ (as listed in table 1) . The mixture was mixed for 30 minutes and a homogenuous solution was formed . The casting method was used to produce samples with 8cm diameter and then maintained for 240 hours at room temperature in air until they dried. The film thickness was ranging within 120±5 µm as measured by digital vernier caliper.

Table (1) The purification tabulated of CMC and nanocomposite films

Sample	CMC (g)	NiO (g)	$BaTiO_3$ (g)	Fig milk (g)
CMC	1	0	0	0
CMC/NiO, fig milk and 1 wt.% $BaTiO_3$	0.93	0.03	0.01	0.03
CMC/NiO, fig milk and 2 wt.% $BaTiO_3$	0.92	0.03	0.02	0.03
CMC/NiO, fig milk and 3 wt.% $BaTiO_3$	0.91	0.03	0.03	0.03
CMC/NiO, fig milk and 4 wt.% $BaTiO_3$	0.90	0.03	0.04	0.03

Fourier-transform infrared (FT-IR) spectra using a Bruker Vertex–70 instrument (Germany) were conducted in the range of 500-4000 cm^{-1} to study the functional groups in polymer and its NCs. The transmission and absorption spectra in the wavelength range of 190-1100 nm were recorded at room temperature using a UV-Visible spectrophotometer (Shimadzu UV-1650 PC, Japan).

3. Results and Discussion

The FTIR spectra of the CMC polymer and its NCs containing fig milk, NiO and different weight percentages of $BaTiO_3$ NPs are shown in Fig. (1). FTIR measurements before and after loading on carboxy-methyl cellulose were carried out. The characteristic vibrational bands of nanocomposites mainly include those observed at 2924.73, 1733.65, 1377.30, 1243.17 and 1024.45 cm^{-1}. The broad peak seen at 3363.09 cm^{-1} was caused by –OH stretching, while the peak at 2920 cm^{-1} was caused by asymmetric $–CH_2$ stretching within the CMC particles (Fig. 1).

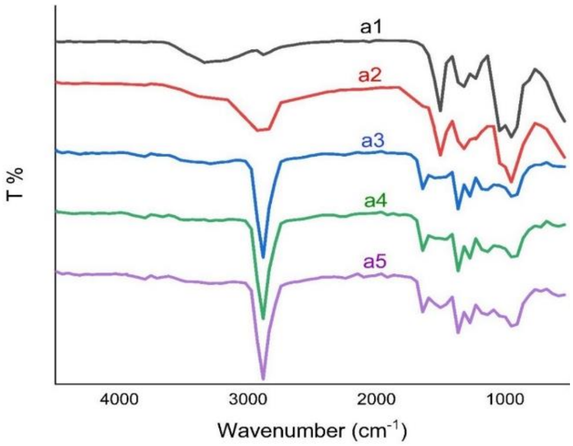

Fig. (1) FTIR spectra of (a1) CMC polymer, (a2) CMC/3wt.% NiO, 3wt.% of fig milk and 1wt.% of $BaTiO_3$, (a3) CMC/3wt.% NiO, 3wt.% of fig milk and 2wt.% of $BaTiO_3$, (a4) CMC/3wt.% NiO, 3wt.% of fig milk and 3wt.% of $BaTiO_3$, and (a5) CMC/3wt.% NiO, 3wt.% of fig milk and 4wt.% of $BaTiO_3$

When the characteristic wavenumbers of the polymer are compared to those of the NCs, it is observed that the addition of varying weight percentages of $BaTiO_3$ NPs has caused a modest shift toward higher wavenumbers, particularly at 1589.06 cm^{-1}. Additionally, when the ratios of $BaTiO_3$ NPs allocated to increase NP density rise, the transmittance falls. This study clearly shows that there are no new absorption peaks and, as a result, no interactions between the polymer matrix and the NPs.

Figure (2) shows optical microscopic images of films of nanocomposites (CMC/NiO – fig milk and different weight percentages of $BaTiO_3$ NPs) at a magnification power of 10X for samples with different concentrations. When the concentration of $BaTiO_3$ increases, the nanoparticles form clumps inside the polymer. At high concentration for $BaTiO_3$ molecules, concentration network paths are formed through which charge carriers are allowed to pass, causing a change in the material properties [2].

The UV-Vis-NIR absorption spectra of the CMC polymer and its NCs with NiO, fig milk, and various weight percentages of $BaTiO_3$ NPs films were conducted in the range of 190-1100nm as shown in Fig. (3). By adding NiO, fig milk, and $BaTiO_3$ NPs, the absorption edge for NCs films was shifted towarsd the longer wavelengths, resulting in a reduction in the energy gap. As may be observed, NC has a substantially larger absorbance than polymer. The reason for this increase in absorbance with weight percentage of nanomaterials is attributed to the absorption of incident light by free electrons [12].

Figure (4) displays the optical transmission spectrum of the CMC polymer and its NCs with 3wt.% NiO, 3wt.% fig milk, and varying weight percentages of $BaTiO_3$. In the visible and near-infrared (NIR) regions, the transmittance of a pure polymer is almost 90%, but when the weight percentage of $BaTiO_3$ NPs increases, it falls off significantly. This results from the surface nature of the film and its absorption. Regardless the cost, the nanocomposite films can be used as medicine storage packaging because of their decreased transmittance towards UV radiation.

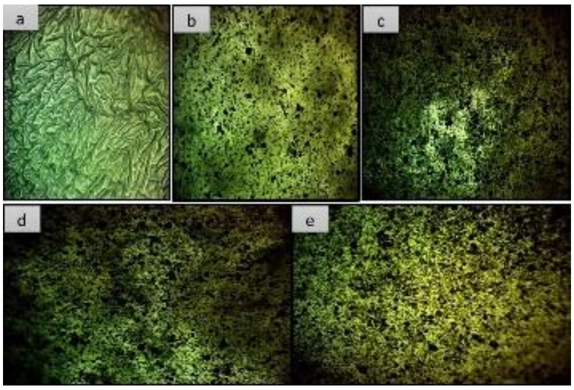

Fig. (2) Microscopic images (10X) for (a) CMC polymer, (b) CMC/3wt.% NiO, 3wt.% of fig milk and 1wt.% of $BaTiO_3$, (c) CMC/3wt.% NiO, 3wt.% of fig milk and 2wt.% of $BaTiO_3$, (d) CMC/3wt.% NiO, 3wt.% of fig milk and 3wt.% of $BaTiO_3$, and (e) CMC/3wt.% NiO, 3wt.% of fig milk and 4wt.% of $BaTiO_3$

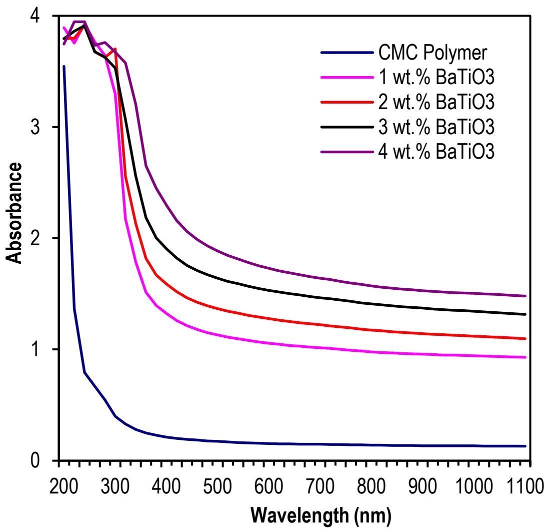

Fig. (3) UV-visible absorption spectra of the CMC and its NCs when combined with fig milk, NiO, and various weight percentages of $BaTiO_3$ NPs

Using Beer-Lambert law, the absorption coefficient (α) as a function of photon energy for the CMC polymer and its NCs films' was calculated [13]:

$$\alpha = 2.303 \ \frac{A}{t} \qquad (1)$$

Absorption levels are minimal at low energy levels, indicating a low probability of electron transition due to the insufficient energy of the incident photon to move the electron from the valence band to the conduction band ($h\upsilon < E_g$). At higher energies, absorption becomes stronger, suggesting a higher probability of electron transitions where the frequency of the incident photon is enough to transfer the electron from the valence band to the conduction band, exceeding the forbidden energy gap. The absorption coefficient helps determine the nature of electron transitions, particularly when the coefficient values are high ($\alpha > 10^4$ cm^{-1}) at high energies, direct electron transitions occur with energy and momentum being maintained by both electrons and photons. When the absorption coefficient values are low ($\alpha < 10^4$ cm^{-1}), indirect transfers occur [14-16].

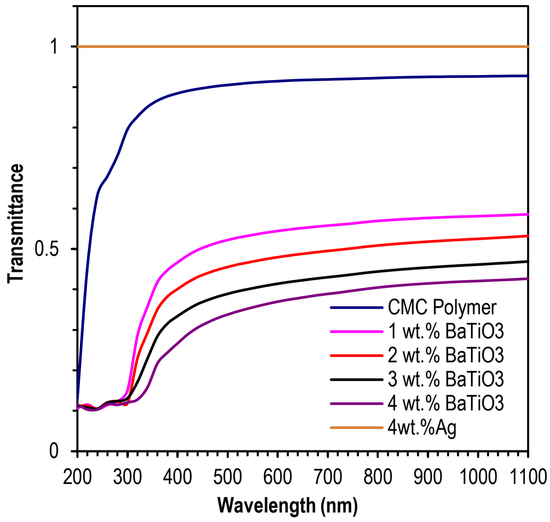

Fig. (4) UV-visible transmission spectra of CMC and its NCs when combined with fig milk, NiO, and various weight percentages of $BaTiO_3$ NPs

The absorption coefficient of the prepared films are low ($\alpha < 10^4$ cm^{-1}) as shown in Fig. (5), which strongly suggests the probability of indirect electronic transitions. At high wavelengths, the absorption coefficient seems lower, which may be connected to the low probability of an electron transition. The electron is absorbed at high energies, which is consistent with earlier research of [7].

As shown in figures (6) and (7), and depending on the absorption coefficient, the optical energy gap can be determined from the plot of $(\alpha h\nu)^{1/r}$ (where r = 2 for allowed and 3 for forbidden indirect transitions) versus photon energy ($h\nu$) using Tauc relation [17] as:

$$\alpha h\upsilon = B(h\nu - E_g^{opt} \pm E_{ph})^r \qquad (2)$$

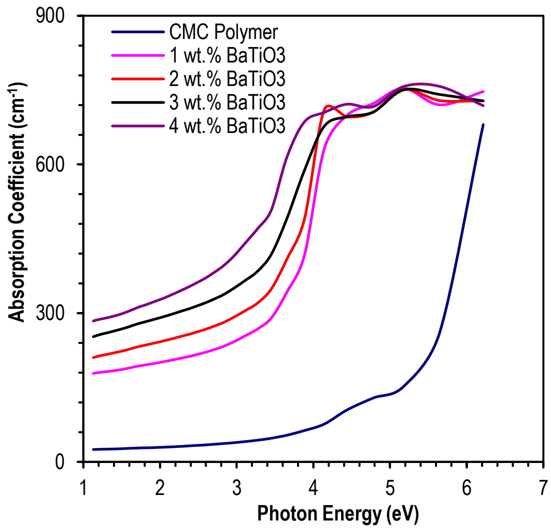

Fig. (5) The absorption coefficient of CMC and its NCs with NiO, fig milk and different weight percentages of $BaTiO_3$ NPs

The indirect energy gap of the CMC polymer was reduced from 4.8 to 1.8 eV for the allowed indirect transition and from 4.4 to 0.6 eV for the forbidden indirect transition after adding nanomaterials.

Table (2) shows the values of the indirect transitions (allowed and forbidden). The indirect energy gap E_g^{opt} is decreased significantly when NiO, fig milk and $BaTiO_3$ NPs are added. This decrease in E_g^{opt} is consistent with findings of other research works [18-20]. The number of ions available for charge transfer is increased by the presence of nickel and barium ions in the as-prepared films, and this causes the inhomogenuous distribution in the film becomes more prevalent. In the energy gap, these dopants also produce energy states. Therefore, the increase in the deformation in the polymer improves the conductivity.

Table (2) Values of E_g^{opt} for indirect transition (allowed and forbidden) of CMC polymer and its NCs

Samples	Allowed E_g (eV)	Forbidden E_g (eV)
CMC	4.8	4.4
CMC/NiO, fig milk and 1 wt.% $BaTiO_3$	3	2.4
CMC/NiO, fig milk and 2 wt.% $BaTiO_3$	2.6	1.8
CMC/NiO, fig milk and 3 wt.% $BaTiO_3$	2.2	1.2
CMC/NiO, fig milk and 4 wt.% $BaTiO_3$	1.8	0.6

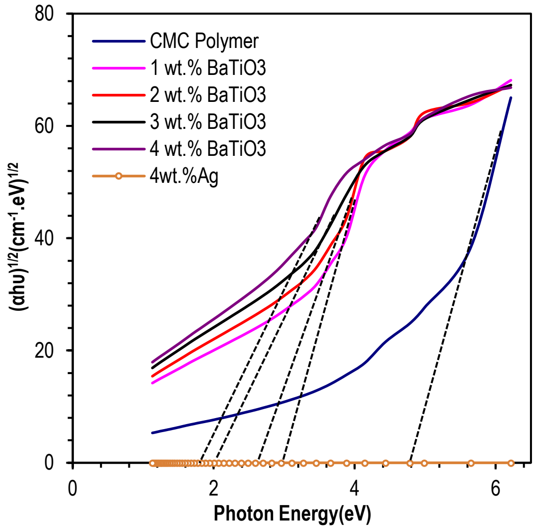

Fig. (6) Relationship between $(\alpha h\nu)^{1/2}$ vs. ($h\nu$) of CMC and its nanocomposites

The refractive index (n), polarizibility (P), and extinction coefficient (k_0) of CMC polymer and its NCs films were determined as [14]

$$n = \frac{1+R}{1-R} + \left[\frac{4R}{(1-R)^2} - k_0{}^2\right]^{\frac{1}{2}} \quad (3)$$

$$P = \frac{3}{4\pi}\left(\frac{n^2-1}{n^2+1}\right) \quad (4)$$

$$k_0 = \frac{\alpha\lambda}{4\pi} \quad (5)$$

The reflectance is denoted by R

It was discovered from Fig. (8) that in the visible and NIR regions, these parameters of NCs films are larger than those of the polymer. The behavior of the polarizability below is correlated with the reduction in refractive index in the UV region.

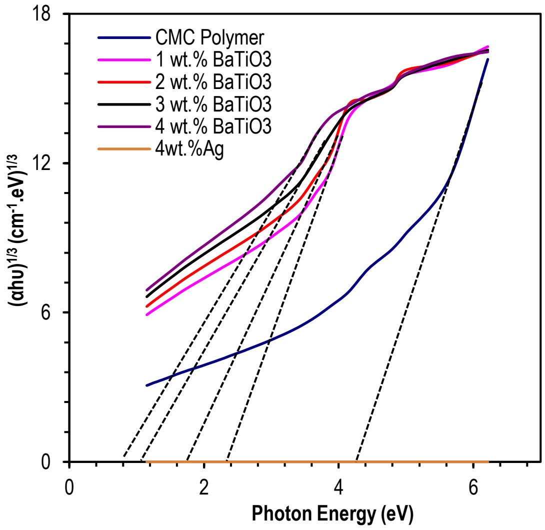

Fig. (7) Correlation between the NCs films of CMC polymer and $(\alpha h\nu)^{1/3}$ vs. ($h\nu$)

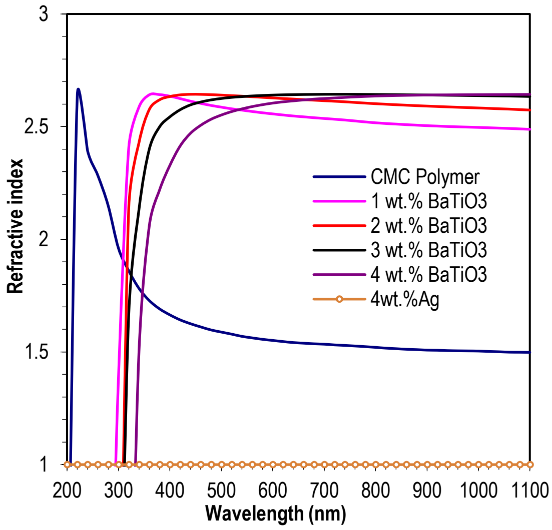

Fig. (8) Variation of refractive index of the NCs films made of CMC polymer containing fig milk, NiO, and varying weight percentages of $BaTiO_3$ NPs

As shown in Fig. (9), the polarizability (P) is directly proportional to the refractive index (n). When materials have a constant speed of light, their refractive index is equal to 1. Because of the electrons shifted to higher levels, polarizability increases with decreasing E_g^{opt}. As a result, the strength of binding to the nucleus is modest, meaning P is larger. When dipoles develop in the UV region, they are unable to keep up with the high frequency (short wavelength), which results in a reduction in polarization. As can be seen in Fig. (10), the extinction coefficient of the nanocomposite films are much higher than that of the CMC polymer. The absorption of light has a direct impact on this finding.

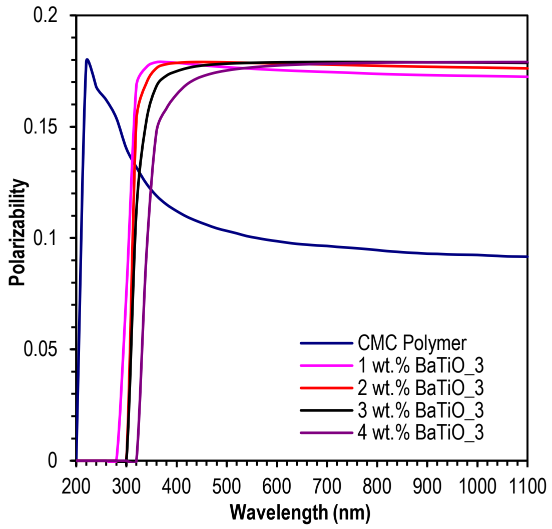

Fig. (9) Variation of polarizability (P) of NCs films made of CMC polymer containing fig milk, NiO, and varying weight percentages of $BaTiO_3$ NPs

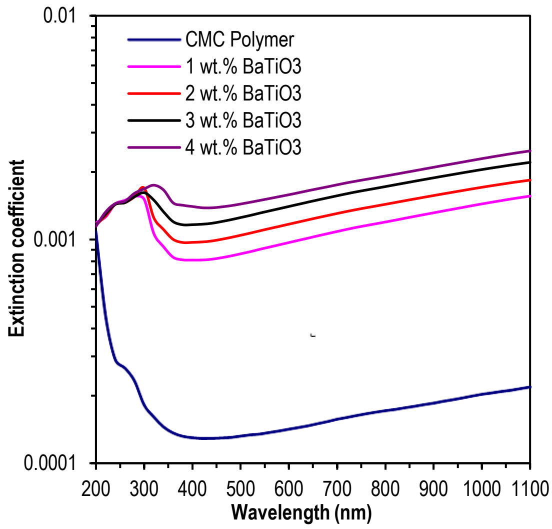

Fig. (10) Variation of extinction coefficient of CMC polymer and the NCs films with incident wavelength

4. Conclusions

CMC/NiO, fig milk, and $BaTiO_3$ films were prepared. The CMC polymer has an optimal transmittance value of 90% in the visible and near-infrared regions. Additionally, when the amount of $BaTiO_3$ NPs in the composite structure is increased, the transmittance drops. High homogeneity and fine distribution of NiO, fig milk and $BaTiO_3$ NPs in the prepared films can be observed by the optical microscopy.

References

[1] S.M. Abdulkadhim, F.S. Hashim and B.H. Rabee, "Synthesis of (PVA-PVP: ZnO and Ag) Nanocomposite Films: Characterization and Antibacterial Application", *NeuroQuantol.*, 20(7) (2022) 738.

[2] A. Hashim et al., "Synthesis and augment structural and optical characteristics of $PVA/SiO_2/BaTiO_3$ nanostructures films for futuristic optical and nanoelectronics applications", *J. Inorg. Organomet. Polym. Mater.*, 34(2) (2024) 611–621.

[3] M.A. Sarabia-Vallejos et al., "Innovation in additive manufacturing using polymers: a survey on the technological and material developments", *Polymers (Basel).*, 14(7) (2022) 1351.

[4] A. Ghaheri, "Characterization of Nanocomposites Synthesized by Al-Si Casting Alloys Reinforced with Silicon Carvide", *Iraqi J. Mater.*, 1(3) (2022) 117-124.

[5] K. Chen et al., "Research progress of intrinsic polymer dielectrics with high permittivity", *IET Nanodielectr.*, 6(4) (2023) 182–211.

[6] A. Hazim, H.M. Abduljalil and A. Hashim, "Design of PMMA doped with inorganic materials as promising structures for optoelectronics applications", *Trans. Electr. Electron. Mater.*, 22(6) (2021) 851–868.

[7] F. Hussain et al., "Polymer-matrix nanocomposites, processing, manufacturing, and application: an overview", *J. Compos. Mater.*, 40(17) (2006) 1511–1575.

[8] J.M. Yaseen, "Crystal Structures and Curie's Temperature of ABO_3 Perovskite Ceramics with Different Ionic Radius", *Iraqi J. Mater.*, 1(2) (2022) 75-82.

[9] C.B. Carter and M.G. Norton, **"Ceramic Materials: Science and Engineering"**, vol. 716, Springer (2007), 159-183.

[10] K.S. Suslick, **"Kirk-Othmer encyclopedia of chemical technology"**, vol. 26, John-Wiley & Sons (NY, 1998), pp. 517–541.

[11] M. Stamataki et al., "Hydrogen gas sensors based on PLD grown NiO thin film structures", *phys. stat. sol.*, 205(8) (2008) 2064–2068.

[12] K.-W. Nam, W.-S. Yoon and K.-B. Kim, "X-ray absorption spectroscopy studies of nickel oxide thin film electrodes for supercapacitors", *Electrochim. Acta*, 47(19) (2002) 3201–3209.

[13] B.H. Rabee, F.Z. Razooqi and M.H. Shinen, "Investigation of optical properties for (PVA-PEG-Ag) polymer nanocomposites films", *Chem. Mater. Res.*, 7 (2015) 103–109.

[14] J.I. Pankove, **"Optical Processes in Semiconductors"**, Courier Corporation, (1975).

[15] K.H.H. Al-Attiyah, A. Hashim and S.F. Obaid, "Fabrication of novel (carboxy methyl cellulose–polyvinylpyrrolidone–polyvinyl alcohol)/lead oxide nanoparticles: structural and optical properties for gamma rays shielding applications", *Int. J. Plast. Technol.*, 23 (2019) 39–45.

[16] A. Hashim, "Enhanced structural, optical, and electronic properties of In_2O_3 and Cr_2O_3 nanoparticles doped polymer blend for flexible electronics and potential applications", *J. Inorg. Organomet. Polym. Mater.*, 30(10) (2020)

3894–3906.
[17] Q.M. Jebur, A. Hashim and M.A. Habeeb, “Structural, electrical and optical properties for (polyvinyl alcohol–polyethylene oxide–magnesium oxide) nanocomposites for optoelectronics applications”, *Trans. Electr. Electron. Mater.*, 20(4) (2019) 334–343.
[18] J. Tauc, A. Menth and D.L. Wood, “Optical and magnetic investigations of the localized states in semiconducting glasses”, *Phys. Rev. Lett.*, 25(11) (1970) 749.
[19] M.M. Abutalib and A. Rajeh, “Influence of ZnO/Ag nanoparticles doping on the structural, thermal, optical and electrical properties of PAM/PEO composite”, *Phys. B Cond. Matter*, 578 (2020) 411796.
[20] K.M.E. Miedzinska, B.R. Hollebone and J.G. Cook, “An assigment of the optical absorption spectrum of mixed valence Co_3O_4 spinel films”, *J. Phys. Chem. Solids*, 48(7) (1987) 649–656.

